AN INTERCOMPARISON EXERCISE ON THE CAPABILITIES OF CFD MODELS TO PREDICT DISTRIBUTION AND MIXING OF H_2 IN A CLOSED VESSEL

Gallego, E.[1], Migoya, E.[1], Martín-Valdepeñas, J.M.[1], Crespo, A.[1], García, J.[1], Venetsanos, A.[2], Papanikolaou, E.[2], Kumar, S.[3], Studer, E.[4], Hansen, O.R.[5], Dagba, Y.[6], Jordan, T.[7], Jahn, W.[8], Høiset, S.[9], Makarov, D.[10], J.Piechna[11]

[1] Escuela Técnica Superior de Ingenieros Industriales, Universidad Politécnica de Madrid, José Gutiérrez Abascal, 2, E-28006 Madrid, Spain
[2] Environmental Research Lab., National Center for Scientific Research "Demokritos", 15310 Aghia Paraskevi, Attikis, Athens, Greece
[3] Building Research Establishment, Fire and Security, Garston, Watford WD25 9XX, UK
[4] Heat Transfer and Fluid Mechanics Laboratory, CEA, F-91191 Gif-sur-Yvette Cedex, France
[5] GexCon, Postbox 6015 Postterminalen, 5892 Bergen, Norway
[6] Explosion-Dispersion Unit, INERIS, Parc Technologique Alata, BP2, F-60550 Verneuil-en-Halatte, France
[7] IKET, Forschungszentrum Karlsruhe, Postfach 3640, 76021 Karlsruhe, Germany
[8] Research Center Juelich, 52425 Juelich, Germany
[9] Norsk Hydro ASA, Corporate Research Centre, P.O.Box 2560, N-3907 Porsgrunn, Norway
[10] FireSERT Institute, University of Ulster, Newtownabbey, BT37 0QB, Northern Ireland, UK
[11]Warsaw University of Technology, Poland

ABSTRACT

This paper presents a compilation and discussion of the results supplied by HySafe partners participating in the Standard Benchmark Exercise Problem (SBEP) V1, which is based on an experiment on hydrogen release, mixing and distribution inside a vessel. Each partner has his own point of view of the problem and uses a different approach to the solution. The main characteristics of the models employed for the calculations are compared. The comparison between results, together with the experimental data when available, is made. Relative deviations of each model from the experimental values are also included. Explanations and interpretations of the results are presented, together with some useful conclusions for future work.

1. INTRODUCTION

As part of the activities within the HySafe Network of Excellence ("Safety of Hydrogen as an Energy Carrier"), experimental tests collected and proposed by the partners of the consortium have been selected for code and model benchmarking in areas relevant to hydrogen safety. Such selected exercises have been identified with the acronym SBEPs –standing for "Standard Benchmark Exercise Problems" – and follow the main objectives for establishing a framework for validation of codes and models for simulation of problems relevant to hydrogen safety, and identifying the main priority areas for the further development of the codes/models.

It was proposed to use existing data to start this activity. Therefore, relevant cases for SBEPs have been selected, based on the relevance to hydrogen safety of the phenomena explored in the tests, the availability and feasibility of the data and their possibility to be used for validating mainly CFD codes.

Comparative assessments of code performance are being made and directions towards further development have been identified. Different codes and models are being assessed by the partners

involved. These tools cover the different approaches used in each phenomenon, i.e. integral, CFD (1D to 3D), in-house, commercial both specific and multi-purpose. Benchmarking exercises should therefore benefit from the complementarities arising from the variety of codes, models, approaches, user experience and points of view from industry and research agents participating in this network. Quality and suitability of codes, models and user practices are being identified by comparative assessments of code results, which constitute the essentials of the SBEPs. Directives towards further development and recommendation for optimal tools and user best practices for phenomena and approaches are to be provided.

A first experiment on hydrogen release, mixing and distribution was selected and identified as SBEP-V1. In the following section, this experiment is described. In the next section, the main characteristics of the models used for the calculations are then briefly compared. Afterwards, the comparison between results and experimental data, when available, is presented. Finally, a discussion about the results is made.

2. EXPERIMENT DESCRIPTION

Shebeko et al. [1] performed hydrogen distribution experiments for a subsonic release of hydrogen in a closed vessel. The flammable volume parameter and similar parameters for amount of reactive gas are useful for risk assessments and ignition probabilities. The geometry of the experimental vessel for simulations in SBEP is shown in Fig. 1a. The vessel fits the major dimensions of the experimental facility, and has a height of 5.5 m, a diameter of 2.2 m, and a volume of 20.046 m^3. At the initial moment, the closed vessel is filled with quiescent air, whose initial temperature was 20°C and the initial pressure 760 mm Hg (101325 Pa). Hydrogen was released vertically upward at the rate of 4.5 litres per second during 60 seconds (0.27 m^3 total), taking into account that the injection tube diameter was 10 mm, the hydrogen release velocity was 57.3 m/s. The release orifice was located on the vessel axis, at 1.4 m under the top of the vessel. It was connected to a supply vessel, whose pressure was about 150 atm. After the release, the sensors were measuring during 250 minutes.

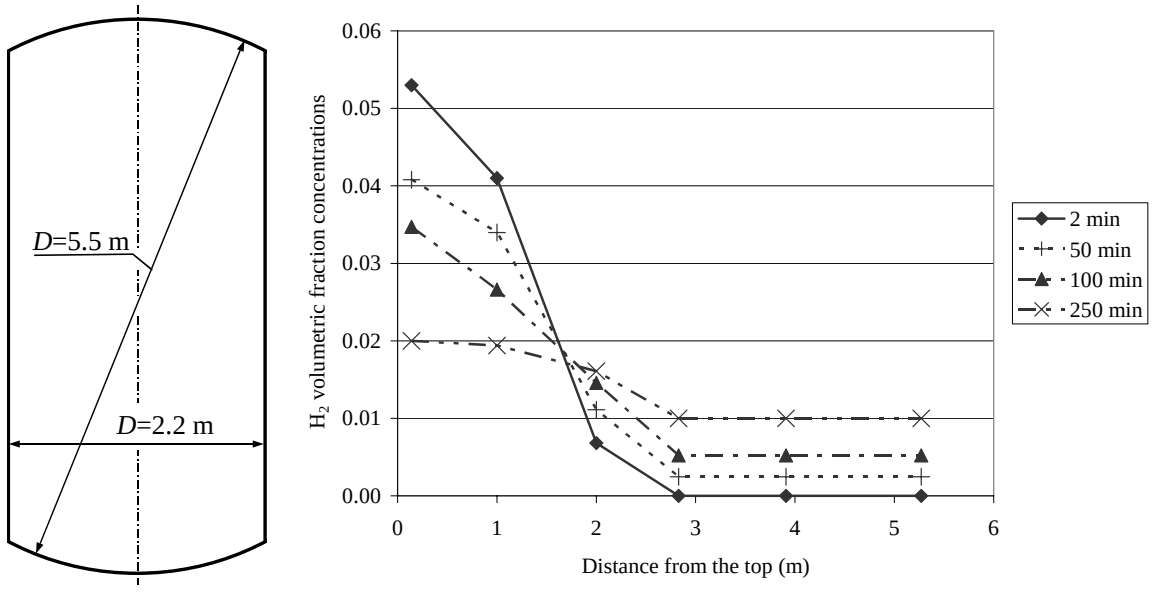

(a) (b)

Figure 1. (a) Shape of the experimental vessel; (b) Distribution of hydrogen concentration along the vessel axis for different times after the hydrogen release.

Six thermo-catalytic gauges were used to measure hydrogen concentration; precision of the concentration measurements was estimated by the authors as ±0.2% of H_2 by volume. Gauges were located at the following distances from the top of the vessel: L_1=0.14, L_2=1.00, L_3=2.00, L_4=2.83, L_5=3.91, L_6=5.27 m. Hydrogen volumetric fraction concentrations along vessel's centreline, recorded during the experiment, are displayed both in Fig. 1b and in table 1. Since the experiment was not repeated, only data from one test is available.

Table 1. Experimental data for comparison with simulation

Gauge No.	Distance from the top of the vessel, m	H_2 vol. concentration (time after completion of 60 seconds release)			
		2 min	50 min	100 min	250 min
1	L_1=0.14 m	5.30E-02	4.08E-02	3.47E-02	2.00E-02
2	L_2=1.00 m	4.10E-02	3.40E-02	2.66E-02	1.94E-02
3	L_3=2.00 m	6.81E-03	1.11E-02	1.46E-02	1.61E-02
4	L_4=2.83 m	0.00E+00	2.47E-03	5.21E-03	1.00E-02
5	L_5=3.91 m	0.00E+00	2.47E-03	5.21E-03	1.00E-02
6	L_6=5.27 m	0.00E+00	2.47E-03	5.21E-03	1.00E-02

3. PARTICIPANTS AND MODELS

One of the most important objectives of the SBEP is to compare the different codes and models. Each participant has used different tools, approaches and assumptions in order to reproduce the experimental data. Some participants used two models or two different approaches. The list of participants and the main characteristics of the models are summarized in tables 2, 3 and 4 in the next pages.

Table 2. List of participants and codes used in the exercise.

Participant Organisations	**Codes**
BRE, Building Research Establishment, UK	**JASMINE 3.2** [2]
CEA, Commissariat à l'Energie Atomique, France	**CAST3M** [3]
DNV, Det Norske Veritas AS, Norway	**FLACSv8.0** [6]
FZK, Forschungszentrum Karlsruhe, Germany	**GASFLOW-II** [4]
FZJ, Research Centre Juelich, Germany	**CFX-5.7** [5]
GXC, GexCon AS, Norway	**FLACSv8.1** [6]
INR, Institut National de l'Environnement Industriel et des Risques (INERIS), France	**PHOENICSv3.5** [7]
NCSRD, National Centre for Scientific Research "Demokritos", Greece	**ADREA-HF** [8]
NH, Norsk Hydro ASA, Norway	**FLACSv8.0** [9]
UPM, Universidad Politécnica de Madrid, Spain	**CFX-4.4** [10]
UU, University of Ulster, UK	**FLUENTv6.1.18** [11]
WUT, Politechnika Warszawska, Poland	**FLUENTv6.1** [11]

Table 3. Main characteristics of the models/codes used by the participants in the exercise.

Participant & Code	**Turbulence model**	**Spatial modelling**	**Discretisation scheme & resolution method** **C = convection terms** **D = diffusion terms** **T = temporal terms**
BRE JASMINE 3.2	k-ε	3D-Cartesian	SIMPLEST pressure-correction C=upwind interpolation D=central-differencing scheme T=first-order fully implicit backward Euler scheme
CEA CAST3M	Mixing length	2D-axysymmetrical and 1D transient pure diffusion	In a first step, momentum and energy are solved using the pressure from previous steps. In a second step, pressure equation is solved using the incremental algorithm. Finite Element discretisation using Q1P0 elements. T=semi-implicit first order incremental projection
DNV FLACSv8.0	k-ε-standard	3D-Cartesian	SIMPLE, second order schemes (C & D) and first order in time (T)
FZK GASFLOW-II	k-ε	2D-axisymmetrical	Phase A: explicit Lagrangian, Phase B: implicit Lagrangian, Phase C: repartition to original grid
FZJ CFX-5.7	k-ε-standard	2D-axisymmetrical	C=high resolution D=high resolution T=second-order backward Euler scheme
GXC FLACSv8.1	k-ε-standard	3D-Cartesian	SIMPLE, second order schemes (C & D) and first order in time (T) Also has possibility for 3^{rd} or 5^{th} order accuracy in C (no point in using this due to coarse grid cells used) and 2^{nd} order in time. Second order time has however proved easily to give instabilities, and is not used as default.
INERIS PHOENICSv3.5	LVEL	2D-axisymmetrical	
NCSRDa ADREA-HF	k-ε-standard	2D-axisymmetrical	C=upwind scheme, D=central differences, T=First order fully implicit
NCSRDb ADREA-HF	LVEL	2D-axi symmetrical	C=upwind scheme, D=central differences, T=First order fully implicit
NH FLACSv8.0		3D-Cartesian	SIMPLE, second order schemes (C & D) and first order in time (T)
UPM CFX-4.4	k-ε	2D-cylindrical symmetry	T=VAN LEER second order except for the energy equation which used CONDIF scheme
UU a & b FLUENTv6.1.18	RNG-LES		Explicit linearization of the governing equations and implicit method for solution of linear equation set C=second order accurate upwind D=central -difference second order
WUT FLUENTv6.1	k-ω and k-ε-realizable	Axisymmetrical	Implicit T=first-order implicit

Table 4. Descriptions of the models used by the participants in the exercise (continuation)

Participant & Code	GRID & Mesh	diffusion coefficient (H_2 in air) & other assumptions	Computer & CPU time
BRE JASMINE 3.2	structured, staggered 90480 cell (29x30x104) minimum grid=2mm, maximum grid=78mm,	0.74 cm^2/s Source 8x8 mm^2	
CEA CAST3M	unstructured 7400 nodes minimum grid=2.7mm, maximum grid=107mm,	0.74 cm^2/s	1 CPU PCs (2.3G§Hz) 1 Gb RAM Linux ~10h CPU
DNV FLACS v8.0	t<75s, 63450 cells (45(x:9-100mm)x47(y:9-100mm)x30(z:200mm)) t>75s, 33408 cells (24(x:100mm)x24(y:100mm)x58(z:100mm))	Source 9x9 mm^2	1 CPU PCs (2GHz) 512-2048Mb RAM Linux t<75s 24 h CPU t>75s 96 h CPU
FZK GASFLOW-II	2420 (1(36º azimuthal)x22(radial)x110(axial)	Source 100 mm diameter Vel=57.3 cm/s	1 CPUs (2.3GHz) 2Gb RAM Linux 7.85h CPU
FZJ CFX-5.7	unstructured 4255 nodes, 12912 tetrahedral elements	0.74 cm^2/s Source 10 mm Vel=57.3 m/s	PC Windows 1.4 GHz Athlon, 1280 MB RAM ca. 15 CPU-days
GXC FLACS v8.1	Structured Fine: t<120s, 80771 cells (10-100mm); t>120s, 33984 cells (100mm), Coarse: t<120s, 4225cells (10-200mm); t>120s, 900 cells (200mm)	Source 10 mm Vel=57.3 m/s Heat transfer to walls (T_{wall}=20ºC)	1 CPU PCs (2GHz) 512-2048Mb RAM Linux Fine(t<120s, 28h CPU, t>120s, 54hCPU), Coarse(t<120s, 1.5hCPU, t>120s, 1.5hCPU)
INERIS PHOENICS v3.5	Staggered grid: scalar variable located at the centre of the control volumes and velocity located on the control volume faces. Minimum grid=2.5mm, maximum grid=120mm, 4400 cells (1(0.1 rad azimuthal) x 44(radial) x 100(axial)	0.7 cm^2/s	1 CPU (2.5GHz) Windows 240Mb RAM 3.8h CPU
NCSRDa & b ADREA-HF	Staggered grid: scalar variable located at the centre of the control volumes and velocity located on the control volume faces Porosity approach. 2071 cell (36(radial: minimum grid 5mm, maximum expansion ratio 1.185, minimum expansion ratio 0.84) x 61(axial: minimum grid 10mm, maximum expansion ratio 1.184, minimum expansion ratio 0.83))	0.61cm^2/s Adiabatic walls	PC Windows
NH FLACS V8.0	Structured Min. grid x y=9mm, z=25mm max. grid x y=150mm, z=100mm 216849 cells	Source 9x9 mm^2	PC Linux 120 seconds during 10 CPU days
UPM CFX-4.4	Unstructured tetrahedral t<180s non-uniform, t>180s uniform fine: 22484 nodes (radial: 2.5-50mm, axial: 25-100mm), coarse: 8944 nodes	Adiabatic walls	1 CPU (2GHz) 1Gb RAM Linux Fine 117h CPU, Coarse 35h CPU
UUa FLUENT v6.1.18	unstructured tetrahedral t<180s non-uniform; t>180s uniform t<180(60+120)s 8714 cell (100-840mm); t>180s 6158 cell (250-350mm)	0.75 cm^2/s Adiabatic walls	t<180: 6 CPU (1.45GHz) 4Gb RAM, 21h CPU t>180s: 2 CPU (1.2GHz) 12Gb RAM,125h CPU
UUb FLUENT v6.1.18	unstructured tetrahedral t<180s non-uniform; t>180s uniform t<180(60+120)s 54004 cell (30-200mm); t>180s 28440 cell (140-200mm)	0.75 cm^2/s Adiabatic walls	6 CPU (1.45GHz) 4Gb RAM t<180, 69h CPU, t>180s, 68h CPU
WUT FLUENT v6.1	12235 cell		1 CPU (3.06GHz) 512 Mb RAM 180 s, 80h CPU

4. RESULTS

It is important to note that for this exercise all details of the experimental results were known to the modellers before the submission. Further, some modellers submitted their results after the initial deadline, with full access to the results predicted in time by other modellers. Since most of the model predictions will strongly depend on user choices (grid, choice of sub-model, etc.) little can be said about prediction capabilities from the simulation performed. Being a first exercise, we were more interested in learning about the strength and limitations of the available models to simulate the phenomena than in the predictive power of each team. Optimally, predictive power should be tested against blind simulations, with no knowledge about experiment results or the predictions of the other modellers when submitting.

The distribution of velocity magnitude along the vessel axis, 30 s after beginning of release, is shown in Fig. 2. FZK modelled a source with 100 mm of diameter and, in order to conserve the hydrogen release, a velocity of 57.3 cm/s. This explains the different velocity pattern. The oscillating behaviour of vertical velocity in UU results is due to visualisation peculiarity. As the UU model uses unstructured grid, the vertical axis crosses control volumes, which have centres positioned at different distances from the axis and which, accordingly, have slightly different vertical component of velocity. Being brought all together on the vertical axis, they make impression of "wiggles".

The distribution of hydrogen volume concentrations in the vessel cross-section, at 2, 50, 100 and 250 minutes after the end of release, is shown in Fig. 3, 4, 5 and 6, respectively, for all the calculations and the experiment. Another way to compare the results and the experiments is presented in Figs. 7 and 8, where the ratio of the calculated (C_p) and measured (C_0) concentration is given at 2 and 250 minutes after the end of release, respectively. In Fig. 7, not all the results are represented, due to the zero value of the experimental concentration in the lower part of the vessel, while some of the calculations (FZK and WUT, for instance) are giving non-negligible values. On the opposite, at 2 m from top, GXC, UPM and BRE results are out of the frame shown due to the low values obtained.

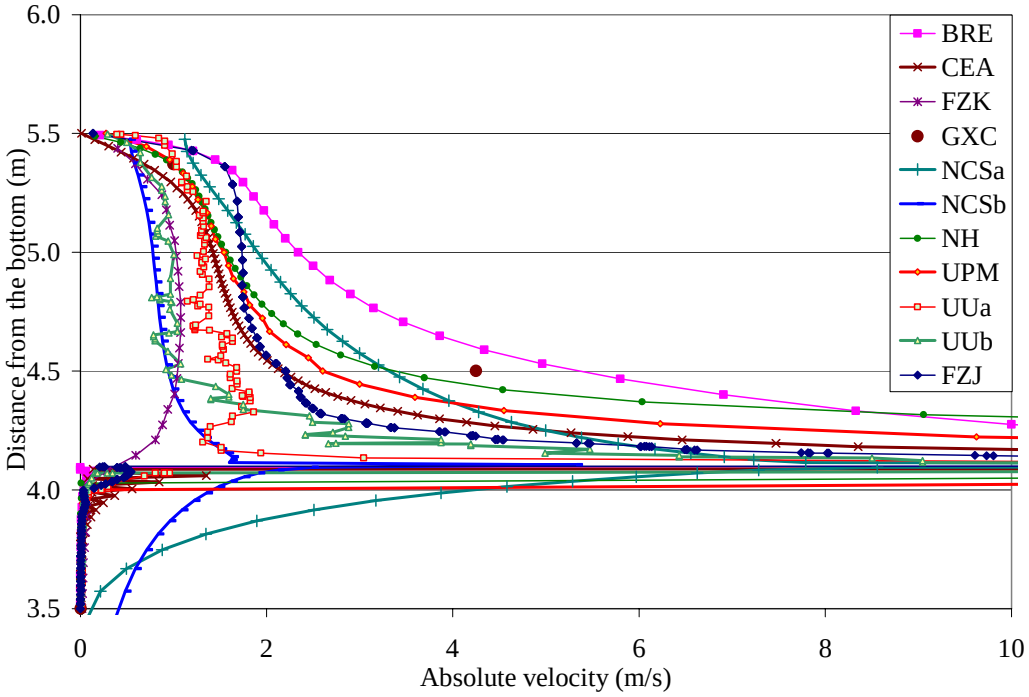

Figure 2. Absolute velocity along the vessel axis at 30s after the beginning of release.

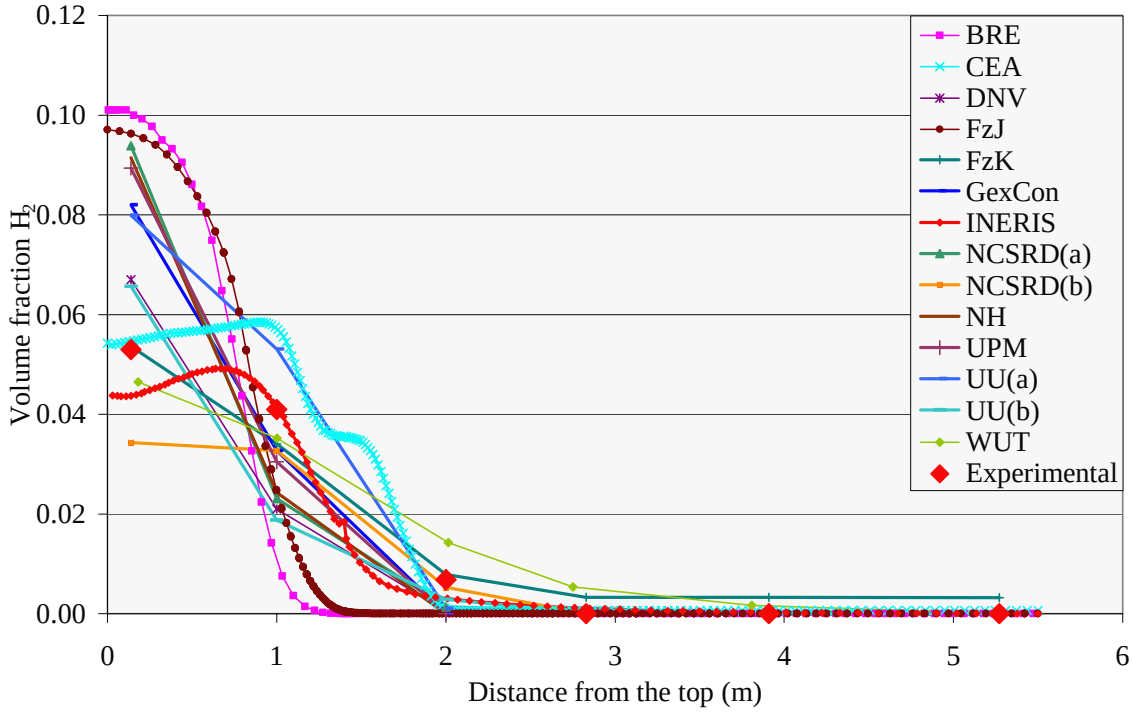

Figure 3. Volume fractions along the vessel centreline (2 min after the end of release)

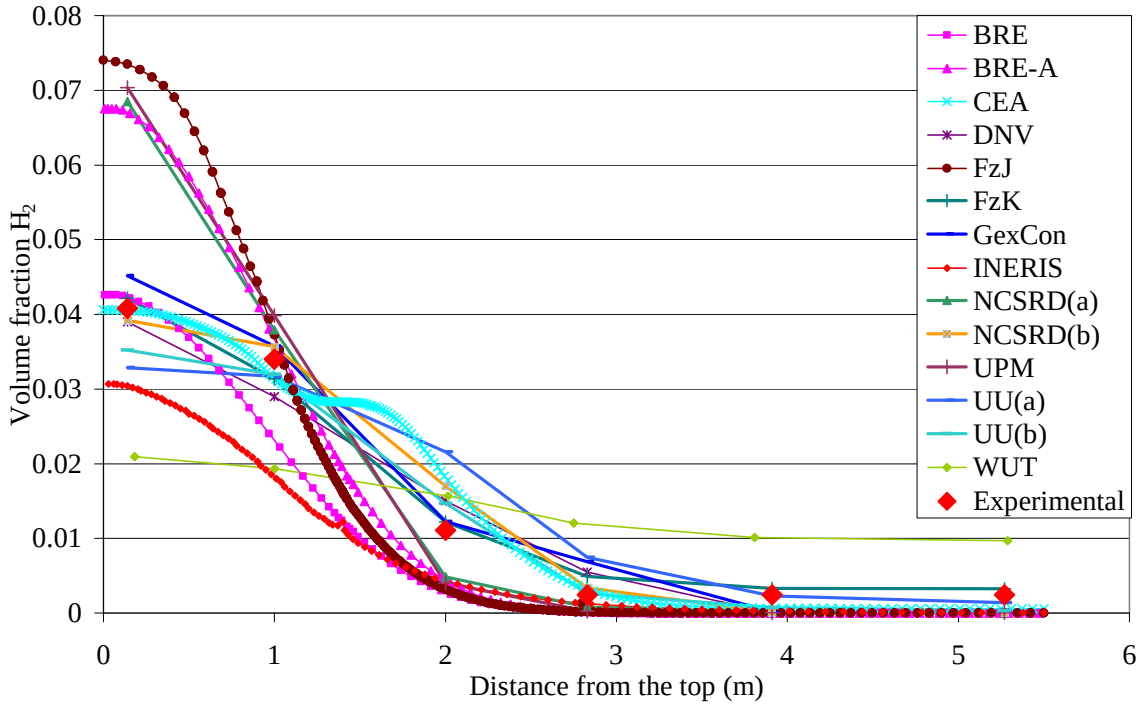

Figure 4. Volume fractions along the vessel centreline (50 min after the end of release)

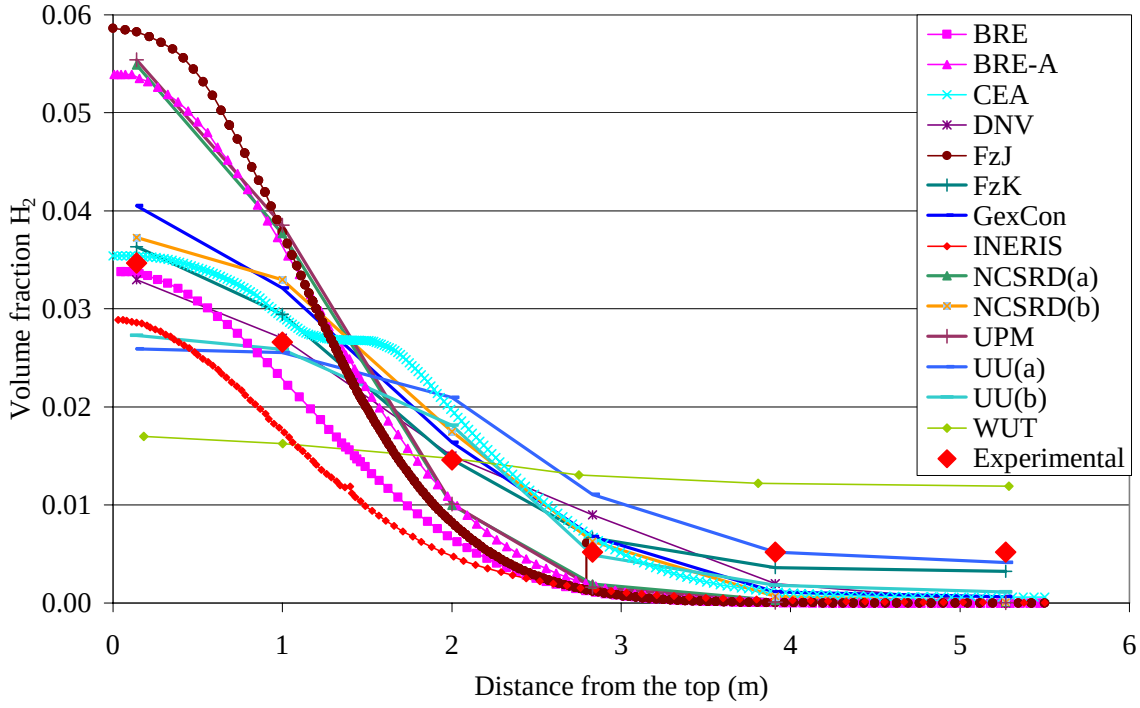

Figure 5. Volume fractions along the vessel centreline (100 min after the end of release)

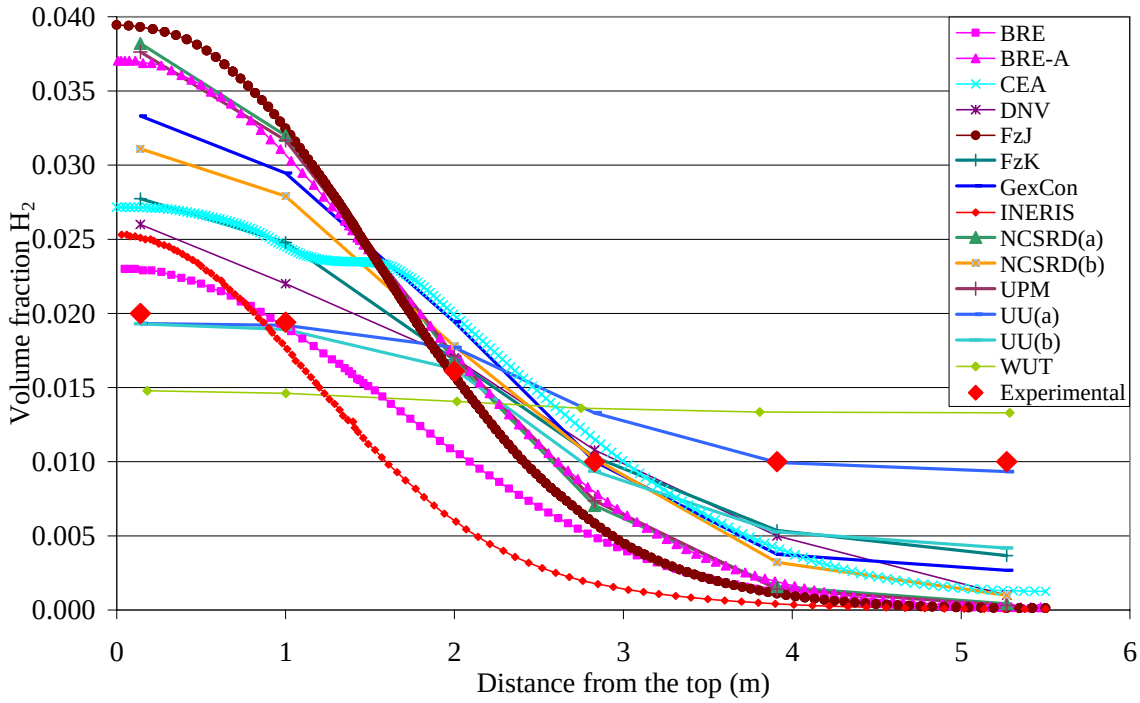

Figure 6. Volume fractions along the vessel centreline (250 min after the end of release)

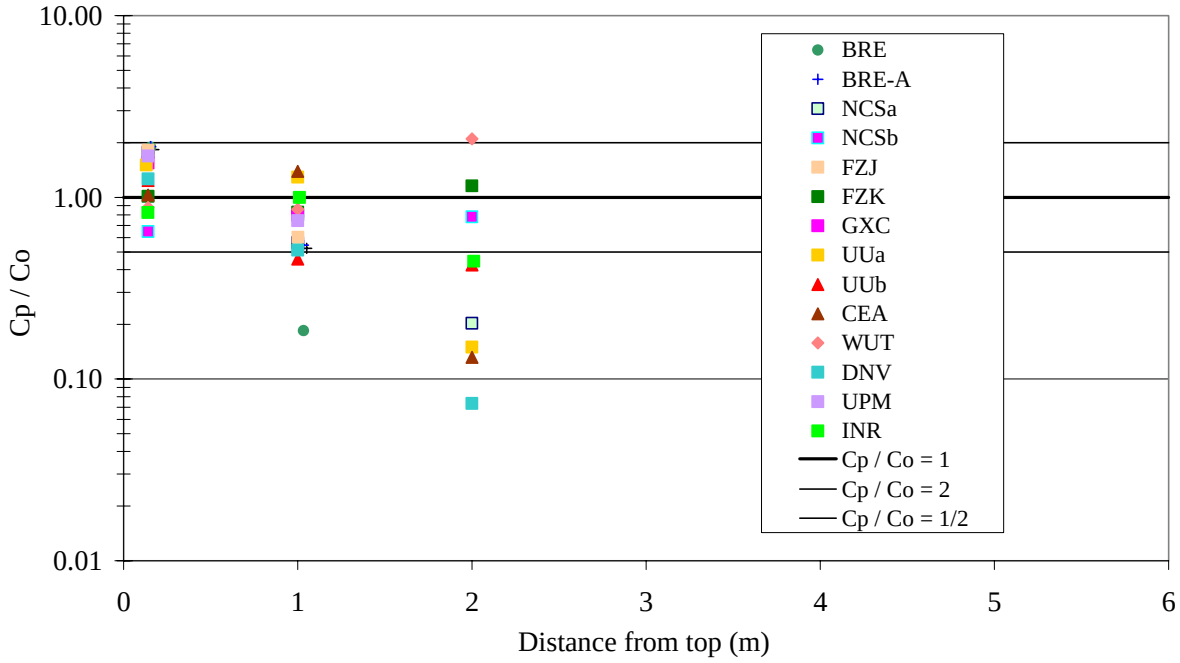

Figure 7. Comparison between models (2 min after the end of release)

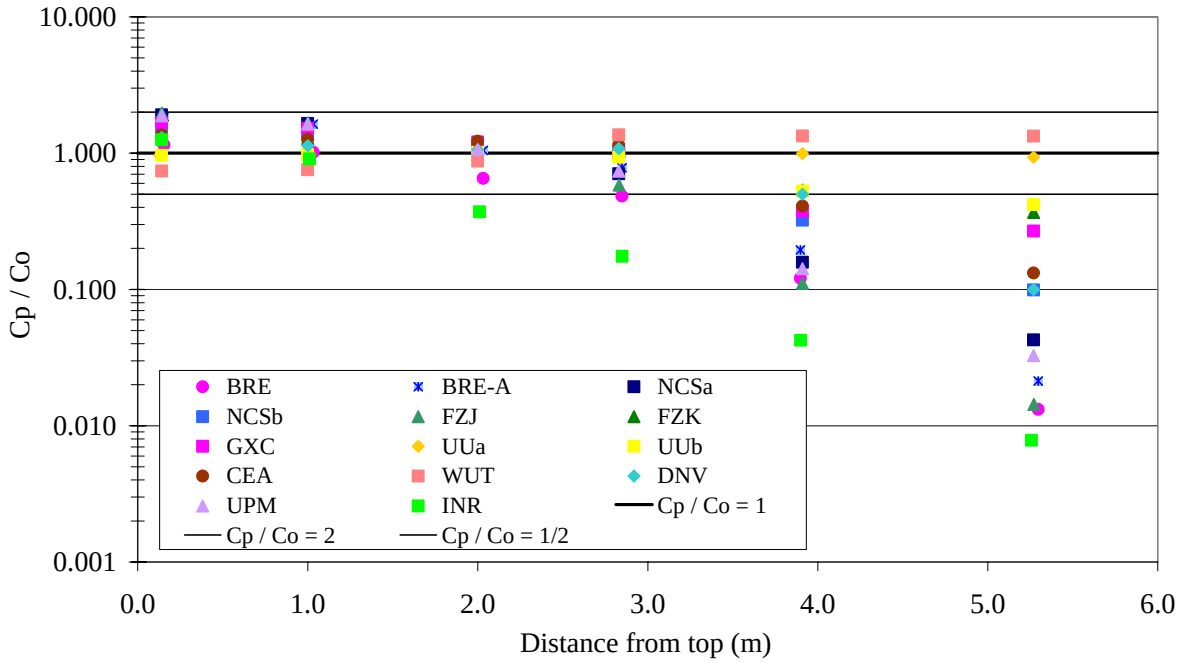

Figure 8. Comparison between models (250 min after the end of release).

5. DISCUSSION

When studying this problem, the following phenomena are relevant, and have been taken into account in the models:

- There is a highly convective region associated to the hydrogen jet, where the ambient gas is entrained and mixes with the hydrogen.
- There is recirculation flow due to the impingement of the jet on the ceiling, that generates wall jets and also produces entrainment and mixing with ambient gas.
- There is natural convection due to non-uniform density distribution because of variable H_2 concentration, and maybe also due to non-adiabatic walls. Because of the variable density and stratifications, there is also a possibility of wave-like motions that have been detected by some models.
- There is mass diffusion, which will be turbulent in the first stages, and maybe laminar in the last ones.

The characteristics of the numerical models are presented in Tables 3 and 4. In some cases, time step and iteration number per time step were set to allow finishing calculations in a reasonable time. As a result, some simulations suffered from low precision, and simulations can be improved using smaller value of the time step. CEA and other partners have performed a grid sensitivity study for this experiment. They have demonstrated that use of too coarse grids can lead to grid-dependent results. Thus, comparison between numerical results and experimental data should only be performed once a grid-convergence study has been made. This is especially important to model dependency issues such as the effect of the turbulence model, where one has to demonstrate that the computed results are driven by the turbulence and not by numerical diffusion due to a coarse grid. For instance, UU(b) results with a finer grid are slightly worse than UU(a). In general, if the grid is not too coarse, the evolution of gas concentration with different grids is very similar.

The comparison between many of the model calculations and measured hydrogen concentration profile reveals significant differences with the general tendency of higher calculated concentrations in the region above the source and lower values below the source. In these models, 2 min after termination of the release, the calculated concentration is almost double as high as the measurement in the top gauge. On the other hand, at that time, no hydrogen was numerically found in the region below the source, whereas some H_2 was registered at the first measuring position below the source. These discrepancies may be explained by a too coarse grid for the source region or, on the experimental side, by a slight asymmetry of the exit flow. Another explanation is that the description of the jet was not sufficiently accurate; besides, there is no information about the measurement equipment and other objects influencing the jet inside the vessel. These discrepancies become somewhat smaller for longer times, so that the H_2 diffusion downwards can be said to be in general well reproduced in the later stages, particularly in UU(a) model. The fact that the measured concentrations in the lower part of the vessel are gradually increasing with time is well reproduced by all models; and the agreement between experiments and model can even be improved by choosing an appropriate Prandtl number. However, the fact that the measured concentrations are identical for the three lower measuring positions is not reproduced in the calculation results.

A comparison of the numerical results with an estimated rough balance of total mass of hydrogen is of interest. If it is assumed that the volume fraction is uniform in horizontal planes, the total mass of H_2 in the tank can be inferred from the data presented in figures 3 to 6. This value has to be 22.6 g, after the end of the H_2 release. A discrepancy may indicate that the boundary condition at the outlet is not properly imposed, the numerical equations do not conserve the hydrogen mass or numerical solution didn't converge. The corresponding values for the experiments and the results of the different models are shown in Table 5. It can be seen that the experiments agree quite well with the expected value.

However some of the model results give values of total H_2 mass 30 or 50 % lower than 22.6 g. This loss of H_2 maybe due either to the numerical model, that is not strictly conservative, or that there are non homogeneities in H_2 concentration in horizontal planes. Maybe, mass was lost at certain time-steps due to poor convergence of the hydrogen mass fraction scalar. BRE believe that by reducing the time-step at these points in the simulation, the mass of hydrogen can be better conserved. BRE-A results have been achieved changing hydrogen concentration using the mass lost in the BRE results.

Table 5. Mass of H_2 (g) after the end of the release. Rough estimates based on monitor point readings and calculations.

Case	2min	50min	100min	250min
Experimental	21.7	21.1	21.3	21.5
BRE	19.4	14.0	13.8	13.6
BRE-A	19.4	22.3	22.0	22.0
CEA	25.4	21.3	21.4	21.4
DNV	16.9	19.8	20.0	19.7
FzJ	22.7	23.2	22.4	21.6
FzK	23.0	22.0	21.8	21.4
GexCon	22.4	22.4	22.2	23.4
INERIS	19.7	11.6	11.3	11.2
NCSRD(a)	22.4	23.2	22.6	22.1
NCSRD(b)	16.0	21.7	21.8	21.7
NH	21.7			
UPM	23.0	23.6	22.8	22.0
UU(a)	24.5	21.2	20.4	20.2
UU(b)	22.0	19.9	19.3	18.9
WUT	23.1	22.0	21.9	21.8

[Note: These data have to be carefully used and are indicated only to provide some tendencies found. For example, in the CEA calculations, the mass balance is exact (22.6 g of hydrogen) during the entire transient because this was a constraint of the modelling.]

Summarising, a first group of four partners (FZJ, BRE-A, UPM and NCSRDa) got very similar results, using the standard k-ε model with adiabatic walls thermal boundary condition, the same source configuration and different CFD codes. The predicted concentration levels were found to be overestimated near the top of the vessel and underestimated near its bottom with respect to the experimental. BRE-A calculations show that while the flow was initially turbulent, once the hydrogen release finished the flow eventually became laminar, and was a diffusion dominated problem. Therefore, this experiment and simulations have raised the issue of whether a single turbulence model, e.g. the 'standard' k-ε model, is suitable for both the turbulent initial release and later diffusion dominated phases. WUT proposes to use k-ω model for the first stages and a k-ε for the diffusion stage.

A second group of three partners (GexCon, FZK and DNV) applied standard k-epsilon turbulence modelling and got results different from the above group. The predicted concentrations levels were improved with respect to the previous group predictions, showing less overestimation near the vessel top and less underestimation near the bottom. In the GexCon simulation wall heat transfer was modelled. Because of the compression by the added gas from the jet the temperature of the gas in the vessel was elevated 1-2 ^{o}K. Assuming that the wall temperature remained constant, a cold draft

downwards along the walls may establish and create a transport of low concentrations of hydrogen to the lower part of the vessel. This was to some extent reproduced in the GexCon simulations (in test simulations ignoring the wall temperature very little gas migrated to the lower parts of the vessel with the laminar diffusivity). Studying the experimental results with a simultaneous smooth increase of concentration in the 3 lower locations, Gexcon strongly believe this is the effect transporting the gas to the lower parts of the vessel. In the experiment there is little information about temperature control of the vessel. Any kind of non-symmetry in temperature or external heat source/sink will contribute to better mixing as observed in the experiments. FZK used adiabatic walls but assumed different conditions at the source: same mass flow rate but 100 times lower velocity. Under these conditions hydrogen has more time to mix with the surrounding air before it reaches the vessel top.

A third category comprises one partner (WUT) who made two simulations using the commercial, multipurpose, code FLUENT, with the k-ω model of turbulence and the realizable version of k-ε model. The predicted results are very different from all above cases. Due to the expected long computation times, a reasonably distributed grid was used, refined in the jet area. For the initial phase, a first calculation was done with the k-ε realizable option. This model was chosen because of known ability to resolve the round jet extension. The standard wall function was used for resolving boundary condition on the walls. The fluid was treated as compressible. Results indicated a hydrogen concentration on the top of the vessel significantly smaller than the experimental. Then, a second simulation was performed using the k-ω turbulence model; in this formulation, the wall boundaries were resolved by the main turbulence model without the help of the wall function. Results of this second model were closer to the experimental data in the initial period (see fig. 3). In both models, gravitational forces were taken into account: as observed in a sensitivity calculation, buoyancy forces neutralized the formation of strong toroidal vortex structures, which could be present even long time after the end of the hydrogen release. For the long term phase, both models generally showed higher diffusivity than observed in the experimental data, probably due to the very crude grid used in the lower part of the vessel.

A fourth group comprises of two partners who applied the LVEL turbulence model (NCSRDb and INERIS) and obtained very different results. The INERIS results underestimate the total hydrogen concentration inside the tank. A reason could be that the filling tube was modelled so the real inlet condition is set at the bottom of the tank. The tube wall is present in the domain during the filling and the diffusion periods. Due to that, the concentration profiles could not be taken on the axis but have been taken at a radius close to the filling tube wall. Another possible reason is that the LVEL model combined with the friction on the tube wall induces a higher hydrogen velocity coming into the tank. This phenomenon accelerates the hydrogen diffusion at the top of the tank. The PHOENICS version used to model this case, does not allow the setting of the inlet condition as a volume source. Better results could be obtained by using volume source with laminar inlet velocity profile as the NCSRDb results show.

A fifth group comprises of one partner (CEA) who used a one-equation turbulence model. The predicted concentration results follow the abovementioned second group general trends. In this case some flattening of the profiles was observed close to the injection level and was attributed to the presence of the injection pipe in the grid. CEA results are in agreement with most of the other computed results, with an underestimation of the time-evolution of hydrogen enrichment in the lower part of the vessel. The flat profiles that are observed in some calculations, as in Fig. 3 for instance, close to the injection level could be due to the presence of the injection pipe in the grid. The benchmark results and a comparison with a CEA solution using pure 1D diffusion model have shown that some other phenomena have an effect on the experimental distribution of hydrogen.

Finally a sixth group comprises of the results obtained by partner UU employing RNG-LES and adiabatic wall boundary conditions. The UU LES model is based on the renormalisation group (RNG) theory and has the advantage of restoring molecular viscosity value, if laminar flow is reached. The

use of unstructured grid is another essential feature of the UU approach as it has been recognised that LES has to be applied on unstructured grids. With adiabatic conditions at the wall boundaries the LES model was able to reproduce a considerable increase of hydrogen concentration at the bottom of the vessel. It looks as though the LES model can reproduce more realistic transport of hydrogen to the bottom compared to the most of RANS models applied. Nevertheless, the transport of hydrogen to the bottom was less pronounced compared to the experiment. This could be attributed to the possible non-uniformity of the vessel wall temperature since the vessel was located at open air. The analysis of UU numerical simulations demonstrated that convective transport of hydrogen dominates over "turbulent" diffusion transport even at times long after the release was completed. It seems that assuming transport of hydrogen mainly by diffusion in such kind of problems is not valid. Indeed, residual chaotic velocities are as high as about 0.10 m/s at 50 min after the release, 0.08 m/s at 100 min and 0.05 m/s at 250 min. This observation should be compared in detail to simulated residual velocities (rms for RANS) to get a deeper insight into the phenomenon of slow transport of hydrogen in closed spaces. "Super" long time of this particular test poses a question about the role of simulation accuracy, which could be controlled through the conservation of hydrogen mass in the calculation domain and the value of residual velocity, on the predicted hydrogen transport.

6. CONCLUSIONS

Different approaches have been used to simulate the experiment. It is difficult to compare the combined effects on simulation results of turbulence model (LES RNG, RANS k-e standard), grid (structured vs. unstructured), size of the grid, the time steps... Comparison between numerical results and experimental data should only be performed once a grid-convergence study has been made, because it is necessary to demonstrate that the computed results are driven by physical phenomena and not by numerical diffusion or inadequate grid resolution.

In general, the simulations have a good agreement with the measurement, but many models have underpredicted the transport of the hydrogen to the bottom region at the beginning, and improved their results at the end. The simulations are better improved using a different Prandtl turbulent numbers during the diffusion. A recommendation for future works is checking conservation of hydrogen (mass) and numerical loss of hydrogen at points of poor convergence. Shorter time steps and stricter convergence criteria could probably guarantee the mass conservation. WUT partner suggested that the simulation should be performed with two different turbulence models, one before and other after the end of the release. In all cases, an appropriate choice of turbulence model must be selected because turbulent flow becomes laminar in a relative short time. Appropriate models should be chosen to simulate hydrogen transport in the last stages, when turbulence velocities are very low.

In the above discussion it was implicitly assumed that the experiments were ideal. This was not the case. Reproducibility was not reported. Temperature at release exit was not reported. Temperature at the walls was not monitored. Information concerning the uncertainty range of the measured data should also have been provided. Some partners also noted that the reported concentration values at the three lowest sensors were suspiciously identical. A partner noted that the sensors above the source were hit by the jet and suggested that these sensors were probably not calibrated for such conditions, adding that this could lead to higher experimental sensor readings and eventually better agreement to the predictions of groups 1 and 2. These issues certainly provide recommendations to experimentalists and future SBEPs.

An important open issue, in order to quantify the convection mixing due to gas heating transport, is the effect of the non-adiabatic walls. Experiments with accurate flow field measurements under adiabatic temperature conditions could shed some light into this problem. Open questions often remained unanswered due to uncontrolled boundary conditions, in particular the configuration of the exit mouth for hydrogen release. A better control of the boundary conditions is a necessary aspect in order to

produce experimental data for benchmark exercises. This has to be a requirement for further SBEP exercises.

However, the performed SBEP simulations provided very useful comparison of performance of different models, which could hardly be possible to conduct by any single partner alone.

This SBEP has revealed one major recommendation for CFD calculations: the CFD modeller must make sure that the hydrogen mass balance is kept at all times. Performed calculations showed that hydrogen mass balance problems occurred when the time steps were too high.

The reasons for hydrogen transport down to the bottom of the vessel remain a gap of knowledge. To improve our understanding of slow hydrogen movement in a closed vessel the further research on flow decay during long period of time is needed.

ACKNOWLEDGMENTS

The authors wish to acknowledge the input received from the following colleagues who contributed to the calculations and the discussions of the results: Stewart Miles (BRE), T. Elvehøy (DNV), J. Travis (FZK), Wilfried Jahn (FZJ), Vladimir Molkov (UU) and A. Teodorczyk (WUT).

This work was supported by the HySafe Network of Excellence *("Safety of Hydrogen as an Energy Carrier"*) of the VI Framework Research Programme of the European Commission (contract no. SES6-CT-2004-502630).

REFERENCES

1. Shebeko, Y.N., Keller, V.D., Yeremenko, O.Y., Smolin, I.M., Serkin, M.A., Korolchenko A.Y., Regularities of formation and combustion of local hydrogen-air mixtures in a large volume, *Chemical Industry*, **21**, 1988, pp. 24(728)-27(731) (in Russian).
2. Cox, G. & Kumar, S., *Field modelling of fire in forced ventilated enclosures*. Combust. Sci. and Tech., 52, 1987, pp. 7-23.
3. Paillère, H. et al., *Simulation of H2 release and combustion in large scale geometries: models and methods*, SNA-2003, SuperComputing for Nuclear Applications, Paris, France, Sept. 2003.
4. Royl, P., Rochholz, H., Breitung, W., Travis J. R. and Necker G., *Analysis of steam and hydrogen distributions with PAR mitigation in NPP containments*. Nuclear Engineering and Design, Vol. 202, Issues 2-3, pp. 231-248, December 2000.
5. http://www.ansys.com/products/cfx.asp
6. Hansen, O.R., Renoult, J., Tieszen, S.R. and Sherman, M., *Validation of FLACS-HYDROGEN CFD Consequence Model Against Large-Scale H_2 Explosion Experiments in the FLAME Facility*, paper to be presented at International Conference on Hydrogen Safety, Pisa 8-10 September, 2005.
7. http://www.cham.co.uk/phoenics/d_polis/d_docs/tr000.htm
8. Bartzis, J. G., *ADREA-HF: A three dimensional finite volume code for vapour cloud dispersion in complex terrain*, EUR report 13580 EN, 1991.
9. Hanna, S.R., Hansen, O.R. and Dharmavaram, S., *FLACS CFD air quality performance evaluation with Kit Fox, MUST, Prairie Grass and EMU observations*, J.Atm.Env. 38, 2004, pp. 4675-4687.
10. AEA Technology plc. *CFX 4.4 Flow Solver User Guide*. CD-ROM. Harwell, UK, 2001.
11. http://fluent.com/software/fluent/ .